

Escape Rates of the Hénon-Heiles System

H.J. Zhao and M.L. Du*

*Institute of Theoretical Physics, Chinese Academy of Sciences,
P.O.Box 2735, Beijing 100080, China*

(Dated: July 15, 2018)

Abstract

A particle in the Hénon-Heiles potential can escape when its energy is above the threshold value $E_{th} = \frac{1}{6}$. We report a theoretical study on the the escape rates near threshold. We derived an analytic formula for the escape rate as a function of energy by exploring the property of chaos. We also simulated the escaping process by following the motions of a large number of particles. Two algorithms are employed to solve the equations of motion. One is the Runge-Kutta-Fehlberg method, and another is a recently proposed fourth order symplectic method. Our simulations show the escape of Hénon-Heiles system follows exponential laws. We extracted the escape rates from the time dependence of particle numbers in the Hénon-Heiles potential. The extracted escape rates agree with the analytic result.

PACS numbers: 05.45.-a, 05.45.Pq, 05.20.-y

Keywords: Chaotic escape, Escape rate, Hénon-Heiles system

*Electronic address: duml@itp.ac.cn

I. INTRODUCTION AND MODEL

Bauer and Bertsch[1] studied the decay laws of chaotic and non-chaotic billiards with windows. They found the number of classical particles remaining inside chaotic billiards decreases exponentially, but no-chaotic billiards decay according to power laws. The results suggest that the exponential law is connected to the chaotic dynamics. However, an exception is the circular billiard, which is integrable but decays exponentially[2]. Experimental studies on the decay laws of an elbow cavity using microwaves have also been reported[3]. We consider the Hénon-Heiles system[4, 5] with the following Hamiltonian

$$\begin{aligned} H &= \frac{1}{2}(p_x^2 + p_y^2) + U(x, y), \\ U(x, y) &= \frac{1}{2}(x^2 + y^2) + x^2y - \frac{1}{3}y^3, \end{aligned} \quad (1)$$

where x and y are the coordinates, p_x and p_y are the momenta. The mass of the particle is set to one for convenience. This system exhibits both regular motion and chaotic motion depending on the energy of the system, and it has been studied from statistical, semiclassical and other perspectives[6, 7, 8, 9, 10]. Recently Brack et al have calculated the density of states above threshold[11], but the escape problem has not been addressed so far.

Numerical studies show the motion of Hénon-Heiles system is regular for $E < 1/12$. When E is greater than $1/12$, the fraction of chaotic region in phase space increases with increasing energy until $E = 1/6$ the whole phase space is chaotic. $E_{th} = 1/6$ is the threshold energy of this system. When $E \geq E_{th}$, a particle in the potential well can escape. Fig. 1 shows the contours of the potential $U(x, y)$. There are three saddle points $P_1(x = 0, y = 1)$, $P_2(-\sqrt{3}/2, -1/2)$ and $P_3(\sqrt{3}/2, -1/2)$. All contours with energy less than $1/6$ are closed. A particle with energy less than $1/6$ always moves inside the closed contour and it remains in the well. The contour with $E = 1/6$ is the equilateral triangle $P_1P_2P_3$. The contours with energies larger than $1/6$ are not closed. There are three openings at the three saddle points. A particle with energy above $1/6$ can escape from the well via the three openings. Because this system is chaotic above threshold, the escape in the Hénon-Heiles system should also follow an exponential law. Assuming $N(0)$ random particles with the same energy in the Hénon-Heiles well at $t = 0$, the number of particles at t will be

$$N(t) = N(0) \exp(-\alpha t), \quad (2)$$

where α is an energy dependent decay rate. The purpose of this article is to verify Eq.(2) and to estimate α for different energies.

II. AN ESCAPE RATE FORMULA

We can derive a formula for the escape rate as a function of energy above threshold by using chaotic property of the Hénon-Heiles system. We draw a line perpendicular to the escape direction through each saddle point, they are line A_1B_1, A_2B_2 and A_3B_3 in Fig. 1. For any energy E above threshold, we define the potential well of the Hénon-Heiles system to be the region restricted by the three disconnected contour lines and the three straight lines A_1B_1, A_2B_2 and A_3B_3 . The motion in the well is assumed to be ergodic because of chaos. The distribution on the energy shell is given generally by $\psi(q, p) = \frac{\delta(E - H(q, p))}{\int dq dp \delta(E - H(q, p))}$, where q, p are the coordinates and momenta[5]. For our two-dimensional system, it is easy to work out the results: the distribution in (x, y) is uniform inside the well, and once the particle's position is given, the magnitude of the momentum is fixed by the Hamiltonian in Eq.(1) and the direction of the momentum is uniformly distributed in $[0, 2\pi]$. We define the energy above threshold $\Delta E = E - E_{th}$. We use θ to represent the direction of momentum relative to the y axis. We use $S(\Delta E)$ to denote the area of the well. Then the distribution in the variables (x, y, θ) can be expressed as $\rho(x, y, \theta) = \frac{1}{2\pi S(\Delta E)}$. Given N particles in the well, the number of particles leaving the well through the opening at the saddle point P_1 in unit time can be written as $N \int dx \int_{-\pi/2}^{\pi/2} d\theta \rho(x, y, \theta) |\mathbf{v}(x, y)| \cos(\theta)$, where the integral in x is along the line A_1B_1 and is restricted to the classical allowed part. We note the three openings of the system are symmetric. Therefore the number of particles leaving the well in unit time from three openings are just three times of the above result. The change of N with respect to t is

$$\frac{dN(t)}{dt} = -3N(t)\rho \int_{-\pi/2}^{\pi/2} \cos(\theta) d\theta \int_{-\sqrt{2\Delta E/3}}^{\sqrt{2\Delta E/3}} \sqrt{2(\Delta E - 3x^2/2)} dx \quad (3)$$

$$= -2\pi\sqrt{3}\Delta E \rho N(t), \quad (4)$$

which gives the escape rate $\alpha(\Delta E) = \frac{\sqrt{3}\Delta E}{S(\Delta E)}$.

There is no analytical formula for the area of the well $S(\Delta E)$. We have applied Monte Carlo method to calculate the area as a function of ΔE . The numerical results are represented by dots in Fig.2. We found the numerical results can be represented vary well by the

quadratic polynomial

$$S(\Delta E) = S_0 + S_1 \Delta E + S_2 (\Delta E)^2 \quad (5)$$

where $S_0 = \frac{3\sqrt{3}}{4}$ is the area of equilateral triangle $P_1 P_2 P_3$. By fitting Eq.(5) to the numerical results in Fig.2 using least squares, we have determined the values for the other two coefficients, $S_1 = 9.656$ and $S_2 = -22.61$. The line in Fig.2 is the fitted quadratic polynomial. We finally have the formula for the escape rate in the Hénon-Heiles system,

$$\alpha(\Delta E) = \frac{\sqrt{3} \Delta E}{S_0 + S_1 \Delta E + S_2 (\Delta E)^2}. \quad (6)$$

Very close to the threshold, a power expansion of Eq.(6) may be useful. Define

$$\alpha(\Delta E) = \sum_1^{\infty} B_i \Delta E^i. \quad (7)$$

The coefficients B_i can be expressed in S_0, S_1 and S_2 . They are $B_1 = \frac{\sqrt{3}}{S_0}$, $B_2 = -\frac{\sqrt{3}S_1}{S_0^2}$, and others can be obtained from the following iteration formula, $B_i = -\frac{S_1 B_{i-1} + S_2 B_{i-2}}{S_0}$, $i = 3, 4, \dots$. The numerical values for the first four coefficients in the power expansion of Eq.(6) are $B_1 = 4/3$, $B_2 = -9.9115$, $B_3 = 96.8743$, and $B_4 = -892.547$. The first term in the power expansion is proportional to ΔE , it gives the scaling of the escape rate in the Hénon-Heiles system just above threshold.

III. NUMERICAL SIMULATIONS

In our numerical simulations of the escape processes, we follow a large number of particles. We monitor the number of particles $N(t)$ remaining in the potential well as a function of time and then extract the escape rate. For any energy above threshold, we initially place $N(0)$ particles in the well according to the distribution $\rho(x, y, \theta) = \frac{1}{2\pi S(\Delta E)}$. This distribution sets the initial conditions for the particles. The trajectory of each particle is then followed by numerically solving the Hamilton's equations. We used two algorithms to integrate Hamilton's equation. Runge-Kutta-Fehlberg (RKF) is the first algorithm[12]. In this algorithm the error in each step can be controlled by setting the relative tolerance and the absolute tolerance. In all our calculations, we set the absolute tolerance to 10^{-9} . The second algorithm (CC) was proposed recently by Chin and Chen[13], it is a fourth order forward symplectic algorithm. It is generally believed that symplectic algorithms are better

and can follow the true dynamics longer because they preserve the symplectic structures of Hamilton's equation. The explicit algorithm for advancing the system forward from t to $t + \epsilon$ is

$$\begin{aligned}
\mathbf{p}_1 &= \mathbf{p}(i) + \frac{1}{6}\epsilon\mathbf{F}(\mathbf{q}(i)) \\
\mathbf{q}_1 &= \mathbf{q}(i) + \frac{1}{2}\epsilon\mathbf{p}_1 \\
\mathbf{p}_2 &= \mathbf{p}_1 + \frac{4}{6}\epsilon\tilde{\mathbf{F}}(\mathbf{q}_1) \\
\mathbf{q}(i+1) &= \mathbf{q}_1 + \frac{1}{2}\epsilon\mathbf{p}_2 \\
\mathbf{p}(i+1) &= \mathbf{p}_2 + \frac{1}{6}\epsilon\mathbf{F}(\mathbf{q}(i+1)).
\end{aligned} \tag{8}$$

Note $\mathbf{F} = -\nabla U$ and $\tilde{\mathbf{F}} = \mathbf{F} + \frac{1}{48}\epsilon^2\nabla(|\mathbf{F}|^2)$ includes an correction to the original force. The time step size ϵ can be varied to control integration errors.

In Fig. 3 we show the two trajectories calculated using the two algorithms. The two trajectories start from the same initial condition: the position is at $(x = 0, y = 0.16)$, the energy is $E = 0.18$, and the direction of momentum is in the positive x-axis. Fig.3(a) is the trajectory obtained using RKF algorithm with relative tolerance 10^{-8} . Fig.3(b) is the trajectory obtained using CC method with a time step size $\epsilon = 0.04$. We have verified the accuracy of both calculations. When the time step size and relative tolerance were reduced further, the trajectories did not show noticeable change. Fig.3(a) and Fig.3(b) show clearly the two trajectories obtained using the two algorithms stay close for some time and then separate. In Fig. 3(a), the particle escapes at $t = 299$, while in Fig.3(b), the particle escapes at $t = 172$. The increased separation of the two trajectories calculated with two different algorithms starting with the same initial condition reflects the difficulty to follow chaotic motions for a long time. Nevertheless we can still extract accurate escape rates as shown below.

A large number of particles are used in the simulations of escape process. For example, we initially put $N(0) = 15326$ particles with the energy $\Delta E = 0.0234$ above threshold according to $\rho(x, y, \theta) = \frac{1}{2\pi S(\Delta E)}$ in the well. We advanced this system by following the trajectory of each particle using RKF method with relative tolerance 10^{-8} . We recorded the number of particles $N(t_i)$ remaining in the well in time step $\Delta t = 0.628$. Fig. 4(a) shows $N(t)$ as a function of time in log-linear scale. Fig. 4(b), Fig. 4(c) and Fig. 4(d) show similar results for different energies. One can see the curves in Fig. 4 in all the cases are almost

straight lines, indicating the escape of Hénon-Heiles system follows exponential laws. For each energy, we can extract the escape rate from the simulated $N(t)$. We used the simulated $N(t)$ from time $t = 0$ to a time when ten percent of the particles have escaped and fitted it to $\ln N(t) = c - \alpha t$ using least squares. The fitted parameter α is the extracted escape rate at the corresponding energy.

We compare in Fig.5 the extracted escape rates and the analytic result in Eq.(6) as a function of energy above threshold. The solid line is from the formula in Eq.(6). The circles are the numerical results from RKF method with a relative tolerance 10^{-8} , the diamonds are the numerical results obtained from CC method (Ref.13) with time step 0.04. We verified the numerical accuracy with smaller tolerance and smaller step size, and we found the results did not change. The dashed line also shows the result of the power expansion of Eq.(6) with only the first four terms. The extracted results from the two algorithms agree well. They also agree with the formula in Eq.(6). The first four terms power expansion is accurate close to threshold, when ΔE is greater than 0.05, it starts to deviate from the analytic result in Eq(6) and from the numerical results.

IV. CONCLUSIONS

We have derived a formula in Eq.(6) for the escape rate of the Hénon-Heiles system. We also simulated the escape process by following a large number of trajectories. We used a symplectic algorithm and a non-symplectic algorithm to advance each particle's trajectory in time. We monitored the number of particles remaining in the potential well in time. We found the escape follow exponential laws similar to the chaotic billiard systems[1]. The extracted escape rates using the two algorithms agree with each other, and they also agree with the analytic rate formula for Hénon-Heiles system in Eq.(6).

ACKNOWLEDGMENTS

This work was supported by NSFC grant No. 90403028.

[1] W. Bauer and G. F. Bertsch, Phys. Rev. Lett. **65**, 2213 (1990).

[2] O. legrand and D. Sornette, Phys. Rev. Lett. **66**, 2172 (1991).

- [3] E. Doron, U. Smilansky and A. Frenkel, Phys. Rev. Lett. **65**, 3072 (1990).
- [4] M. Hénon and C. Heiles, Astro. J. **69**, 73 (1964).
- [5] M.C.Gutzwiller, Chaos in Classical and Quantum Mechanics (Springer, New York, 1990).
- [6] F. G. Gustavson, Astro. J. **71** 670 (1966).
- [7] V. L. Berdichevsky and M. V. Alberti, Phys. Rev. A **44** 858 (1991).
- [8] D. W. Noid and R. A. Marcus, J. Chem. Phys. **67** 559 (1977).
- [9] J.B.Delos and R.T.Swimm, J. Chem. Phys. **47** 76 (1977).
- [10] Zhigang Zheng, Gang. Hu and Juyuan Zhang, Phys. Rev. **E52** 3440 (1995).
- [11] M. Brack, J. Kaidel, P. Winkler, S. N. Fedotkin, arXiv/nlin/0511005
- [12] M. C. W. H. Press, S. A. Teukolsky W. T. Vetterling and B. P. Flannery, Numerical recipes in c: the art of scientific computing (Cambridge University Press, Cambridge ,1988).
- [13] S. A. Chin and C. R. Chen , arXiv/astro-ph/0304223.

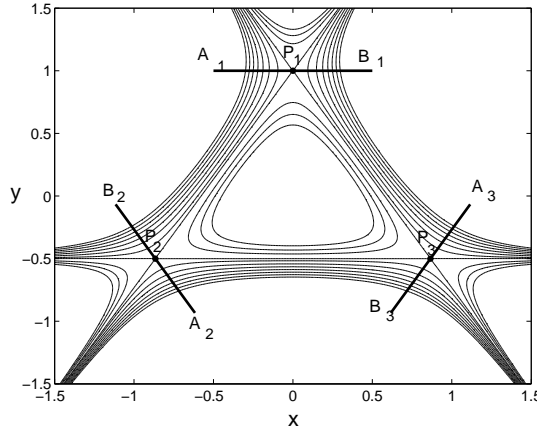


FIG. 1: Equipotential lines of the function $U(x,y)$ in Eq.(1). The points P_1, P_2 and P_3 are saddle points.

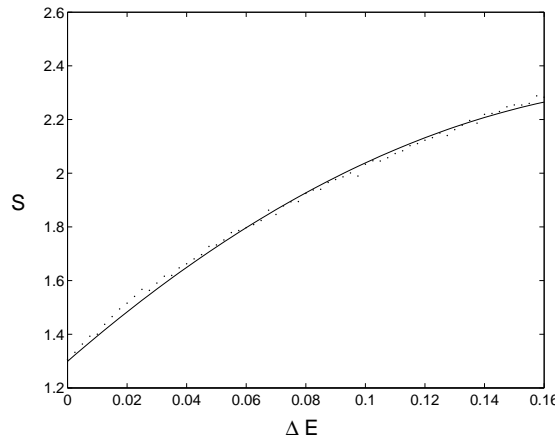


FIG. 2: The area of the well (region bounded by the three disconnected contour lines and the three straight lines A_1B_1, A_2B_2 and A_3B_3) as a function of energy above threshold ΔE . The dots are results calculated using Monte Carlo method. The solid line is the fitted quadratic polynomial in Eq.(5).

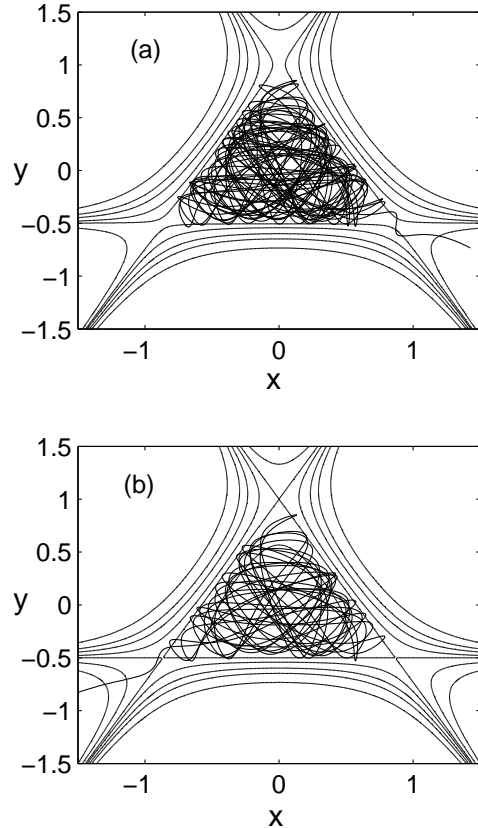


FIG. 3: Trajectories calculated from the two algorithms in the Hénon-Heiles system. Both trajectories start from the position ($x = 0, y = 0.16$) with energy $E = 0.18$, the initial direction of momentum points to positive x-axis. (a) RKF method (Ref.12) with relative tolerance 10^{-8} and time range (0-299). (b) CC method of Chin and Chen (Ref.13) with step 0.04 and time range (0-172).

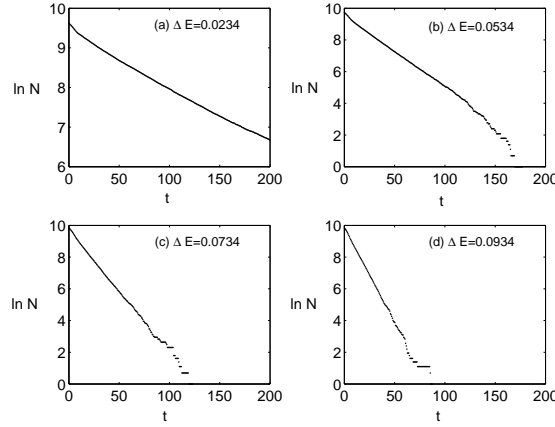


FIG. 4: The number of particles in the well as a function of time for four energies above threshold. (a) $\Delta E = 0.0234$, $N(t = 0) = 15326$; (b) $\Delta E = 0.0534$, $N(t = 0) = 17392$; (c) $\Delta E = 0.0734$, $N(t = 0) = 18885$; (d) $\Delta E = 0.0934$, $N(t = 0) = 19942$. The dots are numerical results obtained using RKF method with a relative tolerance 10^{-8} .

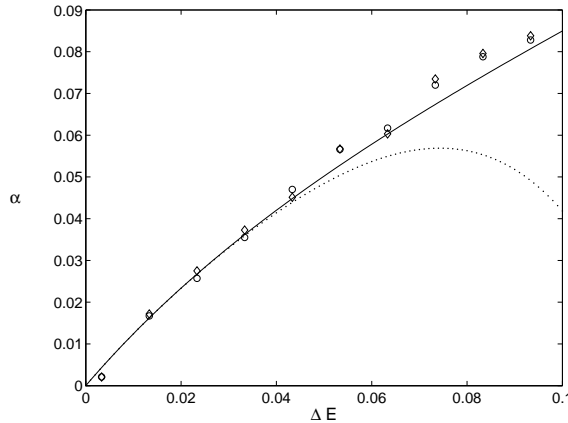


FIG. 5: The escape rate α vs ΔE . The solid line is the formula in Eq.(6). The circles are the numerical results from RKF method with a relative tolerance 10^{-8} , and the diamonds are the numerical results obtained from CC method with a time step 0.04. The dotted line is the power expansion of Eq.(6) with the first four terms.